

Limited Regional Aerosol Changes Despite Unprecedented Decline in Nitrogen Oxide Pollution During the February 2020 Coronavirus Shutdown in China

Michael S. Diamond & Robert Wood

Department of Atmospheric Sciences, University of Washington, Seattle, USA

Contents of this file

Figures S1 to S8
Tables S1 to S3

Introduction

This file contains supporting information documenting:

- Diagnostics for the regression analysis including time series of the regressors (Figure S1); coefficients of determination, RMS errors, and the number of valid datapoints used for each target variable (Figure S2); and the intercepts and regression coefficients for $\ln(\text{NO}_2)$ (Figure S3), AOD (Figure S4), and r_e (Figure S5)
- The time series of PBL SO_2 , averaged over the same region as $\ln(\text{NO}_2)$ and AOD in Figure 3 and excluding major volcanic events (Figure S6)
- Meteorological anomalies during February 2020 (Figure S7)
- Accumulated growth rates through March 2020 (as compared to 2019) for each of the economic indicators shown in Figure 4 (Figure S8)
- NO_x , $\text{PM}_{2.5}$, and SO_2 emissions summed over the region indicated in Figure 5 for the transportation sectors (Table S1), industry and power sectors (Table S2), and other sectors (Table S3)

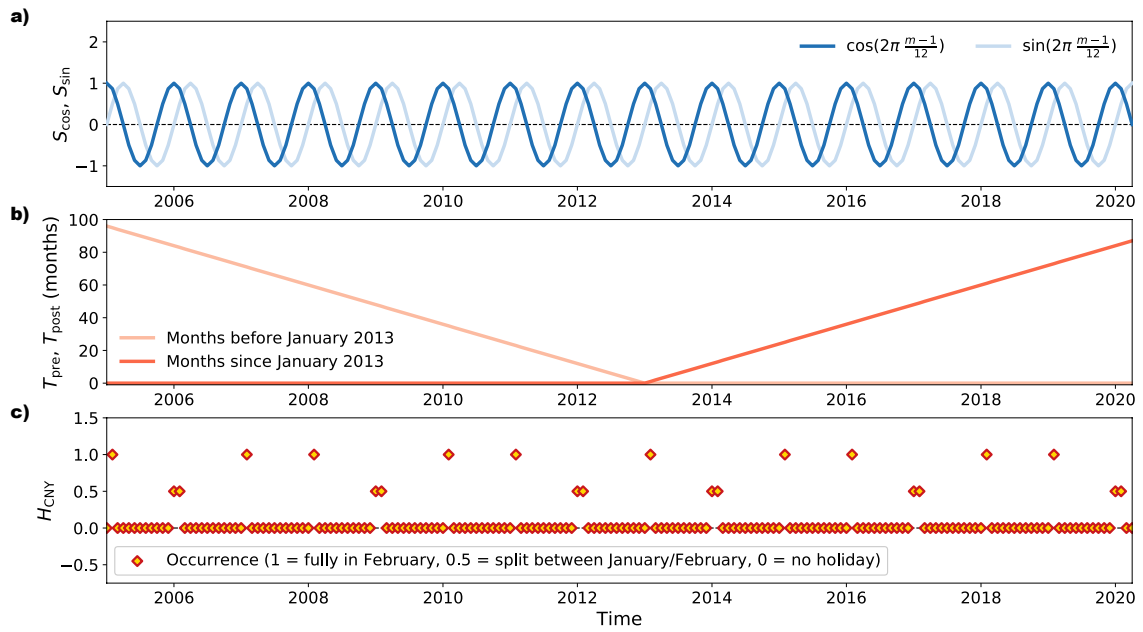


Figure S1. Time series of regressors. **a)** Seasonal cycles S_{\cos} and S_{\sin} . **b)** Trends for the time period before (T_{pre}) and after (T_{post}) January 2013. **c)** Holiday effect H_{CNY} defined as full or partial occurrence of Chinese New Year festivities in a given month.

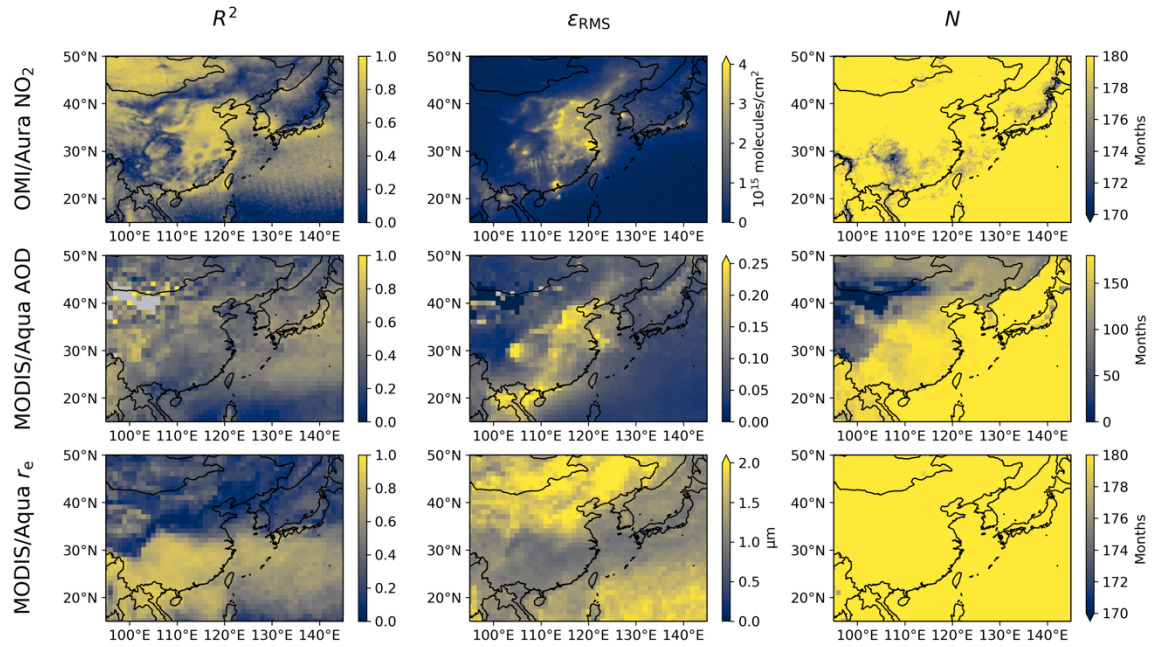


Figure S2. Maps of regression diagnostics. Coefficient of determination (right), RMS error (center), and number of valid data points on which the regression at each grid box was trained (left) are shown for OMI-retrieved tropospheric column NO₂ (top) and MODIS-retrieved aerosol optical depth (middle) and liquid cloud effective radius (bottom). All diagnostic values are calculated for data between January 2005 and December 2019 only.

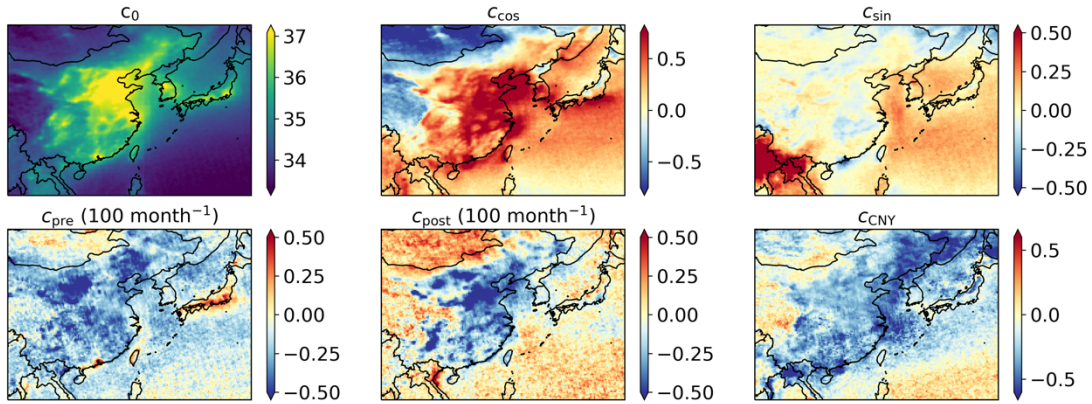


Figure S3. Maps of the regression intercept and coefficients for $\ln(\text{NO}_2)$ from OMI/Aura.

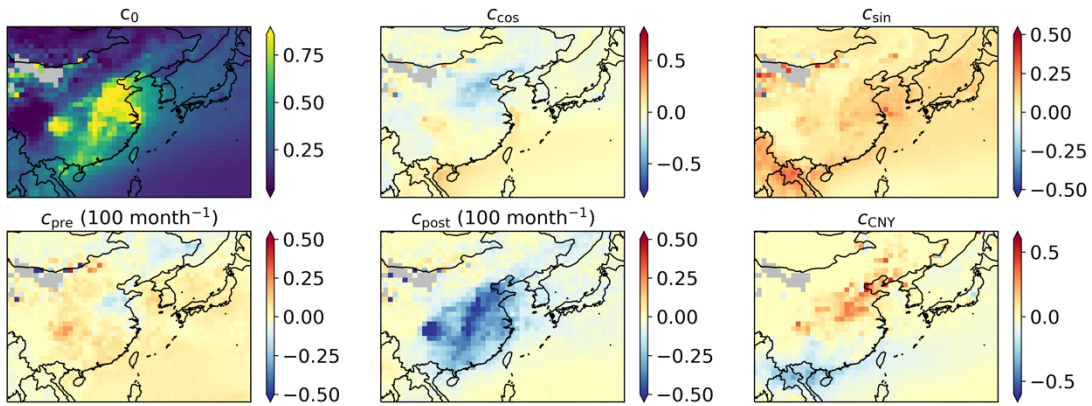


Figure S4. Maps of the regression intercept and coefficients for AOD from MODIS/Aqua.

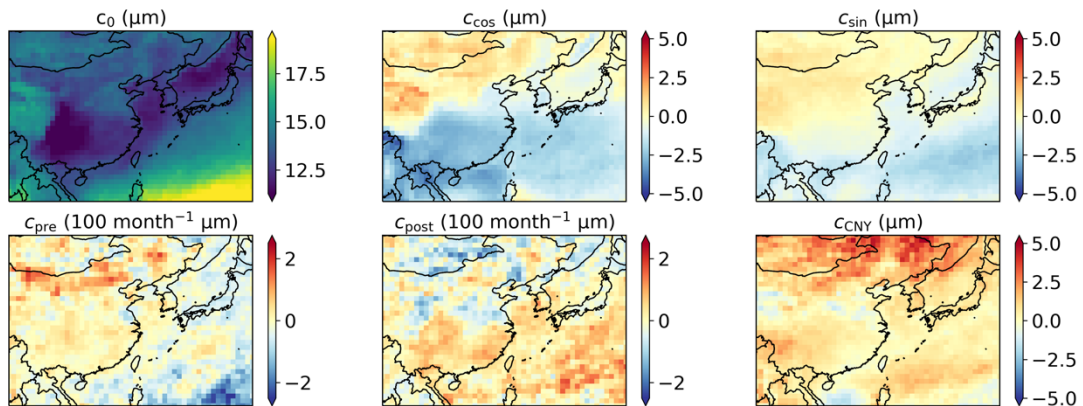


Figure S5. Maps of the regression intercept and coefficients for r_e from MODIS/Aqua.

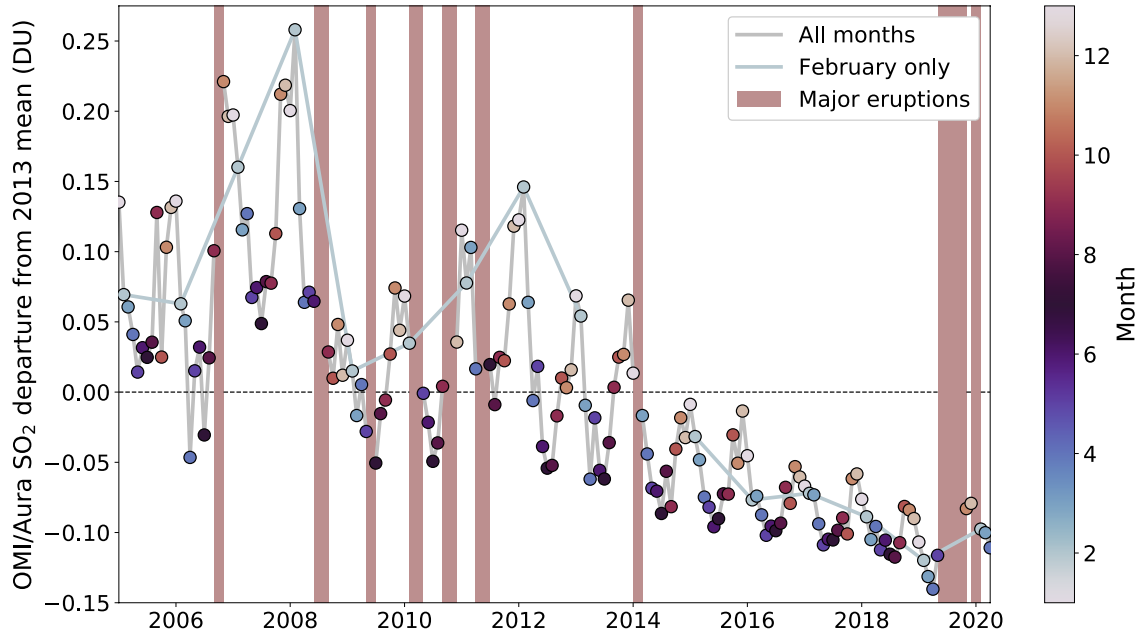


Figure S6. Time series of OMI/Aura planetary boundary layer sulfur dioxide column departures from the 2013 mean averaged over the region 20-42°N, 108-125°E (box in Figure 2ab). Marker colors refer to month and separate lines are plotted for all valid data (gray) and only data for February of each year (light blue). Data potentially affected by volcanic plumes are excluded (shading). The major Northern Hemisphere eruption events that were excluded include:

- October 2006: Rabaul, Papua New Guinea
- July 2008: Okmok, United States
- August 2008: Kasatochi, United States
- June 2009: Sarychev, Russia
- March-April 2010: Eyjafjallajökull, Iceland
- October-November 2010: Merapi, Indonesia
- May 2011: Grímsvötn, Iceland
- June 2011: Nabro, Eritrea
- February 2014: Kelud, Indonesia
- June 2019: Raikoke, Russia
- July 2019: Ulawun, Papua New Guinea
- August-October 2019: Sheveluch, Russia
- January 2020: Taal, Philippines

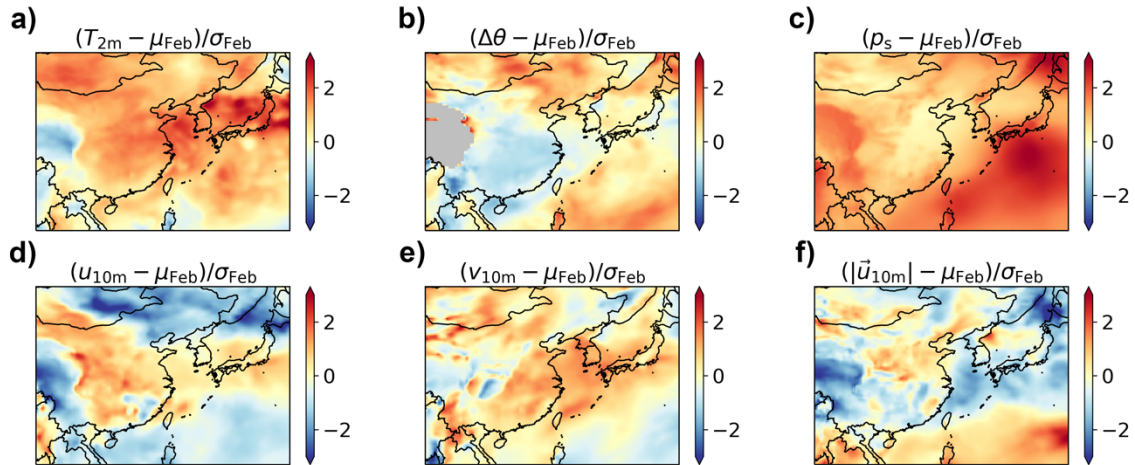


Figure S7. Maps of meteorological anomalies during February 2020. Anomalies are defined as the difference between the February 2020 MERRA-2 field and the 2005-2019 February mean (μ_{Feb}) normalized by the standard deviation (σ_{Feb}) of the 2005-2019 February values for **a)** 2-meter temperature (T_{2m}), **b)** lower tropospheric stability ($\Delta\theta$) defined as the difference between the 700 hPa potential temperature and the 2-m potential temperature, **c)** surface pressure (ρ_s), **d)** zonal 10-m wind (u_{10m}), **e)** meridional 10-m wind (v_{10m}), and **f)** 10-m wind speed ($|\vec{u}_{10m}|$).

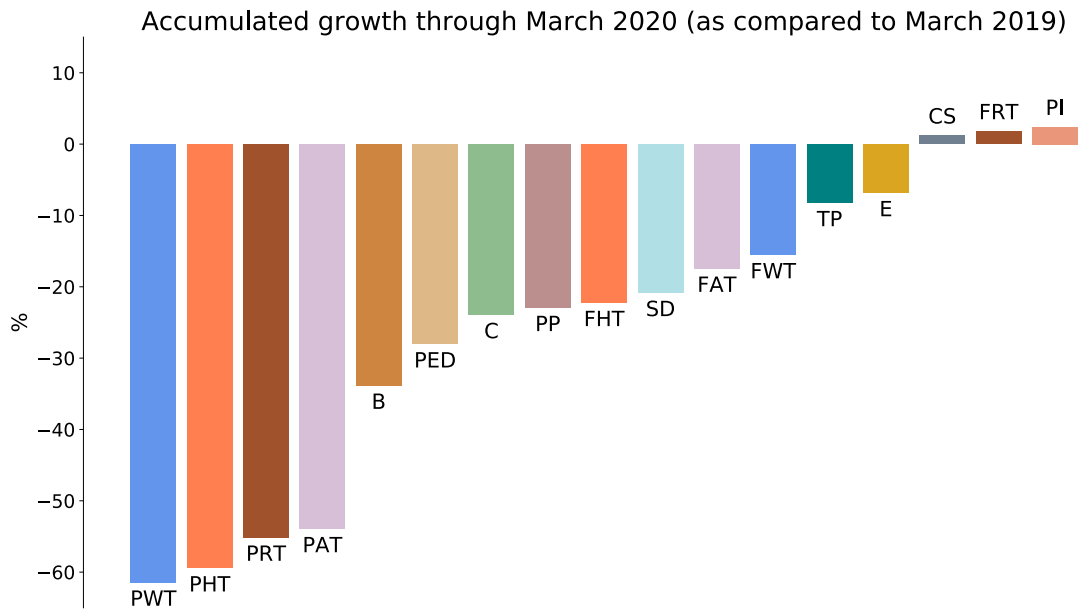


Figure S8. Comparison of the accumulated growth rate through March 2020 (as compared to the accumulated production through March 2019) for each economic sub-sector shown in Figure 4. Bar colors for each economic sub-sector are the same as the line colors in Figure 4. Abbreviations of the sub-sector names are as follows:

- PWT = Passenger Waterway Traffic
- PHT = Passenger Highway Traffic
- PRT = Passenger Rail Traffic
- PAT = Passenger Air Traffic
- B = Beer
- PED = Portable Electronic Devices
- C = Cement
- PP = Plastic Products
- FHT = Freight Highway Traffic
- SD = Soft Drinks
- FAT = Freight Air Traffic
- FWT = Freight Waterway Traffic
- TP = Thermal Power
- E = Electricity
- CS = Crude Steel
- FRT = Freight Rail Traffic
- PI = Pig Iron

Transportation sectors (IPCC 2006 code)	NO _x emissions		PM2.5 emissions		SO ₂ emissions	
	Mass (Tg)	Fraction of total	Mass (Tg)	Fraction of total	Mass (Tg)	Fraction of total
Aviation climbing & descent (1A3a_CDS)	0.089	0.4%	0.002	0.0%	0.008	0.0%
Aviation cruise (1A3a_CRS)	0.102	0.5%	0.002	0.0%	0.009	0.0%
Aviation landing & takeoff (1A3a_LTO)	0.028	0.1%	0.000	0.0%	0.003	0.0%
Road transportation no resuspension (1A3b_noRES)	3.668	17.8%	0.124	1.4%	0.046	0.2%
Road transportation resuspension (1A3b_RES)	0.000	0.0%	0.030	0.3%	0.000	0.0%
Railways, pipelines, off-road transport (1A3c+1A3e)	0.225	1.1%	0.032	0.4%	0.039	0.2%
Shipping (1A3d)	1.274	6.2%	0.218	2.5%	0.829	3.2%
Transportation sub-total	5.387	26.2%	0.407	4.7%	0.934	3.6%

Table S1. Emissions from the transportation sectors over the region 20-42°N, 108-125°E (box in Figure 5) for 2015 from the EDGAR emissions database. Values are reported as the total mass emitted by each sub-sector for the year and what fraction of the total emissions of each species this comprises.

Industry & power sectors	NO _x emissions		PM _{2.5} emissions		SO ₂ emissions	
	Mass (Tg)	Fraction of total	Mass (Tg)	Fraction of total	Mass (Tg)	Fraction of total
(IPCC 2006 code)						
Chemical processes (2B)	0.044	0.2%	0.028	0.3%	0.560	2.2%
Combustion for manufacturing (1A2)	7.353	35.7%	3.938	45.2%	14.428	56.3%
Energy for buildings (1A4+1A5)	0.775	3.8%	1.930	22.2%	1.582	6.2%
Fossil Fuel Fires (5B)	0.006	0.0%	0.023	0.3%	0.049	0.2%
Fuel exploitation (1B1a+1B2aii2+1B2aiii3+1B2bi+1B2bii)	0.002	0.0%	0.001	0.0%	0.000	0.0%
Iron and steel production (2C1+2C2)	0.004	0.0%	0.160	1.8%	0.002	0.0%
Non-ferrous metals production (2C3+2C4+2C5+2C6+2C7)	0.011	0.1%	0.018	0.2%	0.171	0.7%
Non-metallic minerals production (2A)	0.000	0.0%	0.824	9.5%	0.000	0.0%
Oil refineries and Transformation industry (1A1b+1A1ci+1A1cii+1A5biii+1B1b+1B2aiii6+1B2bii3+1B1c)	0.916	4.4%	0.869	10.0%	1.622	6.3%
Power industry (1A1a)	5.786	28.1%	0.286	3.3%	5.952	23.2%
Solvents and products use (2D3+2E+2F+2G)	0.000	0.0%	0.0	0.0%	0.000	0.0%
Industry & power sub-total	14.897	72.3%	8.077	92.8%	24.367	95.1%

Table S2. Emissions from the industry and power sectors over the region 20-42°N, 108-125°E (box in Figure 5) for 2015 from the EDGAR emissions database. Values are reported as the total mass emitted by each sub-sector for the year and what fraction of the total emissions of each species this comprises.

Other sectors (IPCC 2006 code)	NO _x emissions		PM2.5 emissions		SO ₂ emissions	
	Mass (Tg)	Fraction of total	Mass (Tg)	Fraction of total	Mass (Tg)	Fraction of total
Agricultural soils (3C2+3C3+3C4+3C7)	0.223	1.1%	0.032	0.4%	0.000	0.0%
Agricultural waste burning (3C1b)	0.013	0.1%	0.028	0.3%	0.002	0.0%
Food and Paper (2H)	0.013	0.1%	0.008	0.1%	0.293	1.1%
Manure management (3A2)	0.046	0.2%	0.057	0.6%	0.000	0.0%
Solid waste incineration (4C)	0.019	0.1%	0.095	1.1%	0.018	0.1%
Solid waste landfills (4A+4B)	0.000	0.0%	0.000	0.0%	0.000	0.0%
Other sub-total	0.314	1.5%	0.219	2.5%	0.313	1.2%

Table S3. Emissions from other sectors not included above—mainly agriculture and waste management—over the region 20-42°N, 108-125°E (box in Figure 5) for 2015 from the EDGAR emissions database. Values are reported as the total mass emitted by each sub-sector for the year and what fraction of the total emissions of each species this comprises.